

High-pressure phases of uranium monophosphide studied by synchrotron x-ray diffraction

J. Staun Olsen

Physics Laboratory, University of Copenhagen, Universitetsparken 5, DK-2100 Copenhagen, Denmark

L. Gerward

Laboratory of Applied Physics III, Technical University of Denmark, DK-2800 Lyngby, Denmark

U. Benedict and S. Dabos

Commission of the European Communities, Joint Research Centre, European Institute for Transuranium Elements, Postfach 2340, D-7500 Karlsruhe, Federal Republic of Germany

O. Vogt

Eidgenössische Technische Hochschule, Laboratorium für Festkörperphysik, Hönggerberg, CH-8093 Zürich, Switzerland

(Received 18 August 1987; revised manuscript received 14 December 1987)

X-ray diffraction studies have been performed on UP powder for pressures up to 51 GPa using synchrotron radiation and a diamond-anvil cell. At ambient pressure UP has the rocksalt structure. The bulk modulus has been determined to $B_0 = 102(4)$ GPa and its pressure derivative to $B'_0 = 4.0(8)$. The cubic phase has been found to transform to a new phase, UP II, at about 10 GPa. UP II can be characterized by a rhombohedral Bravais lattice. UP II transforms to an orthorhombic phase, UP III, at 28 GPa. No volume change has been observed at the two transitions. The influence of the $5f$ electrons on the transformations is discussed.

I. INTRODUCTION

The present work is part of a series of experiments to study the high-pressure structural behavior of uranium and thorium compounds containing elements from the IV A, V A, and VI A groups of the Periodic Table. UP, like many of these compounds, has the rocksalt structure (B1) at normal pressure and temperature. At low temperature UP is antiferromagnetic, the Néel temperature (T_N) being 123 K. No structural change is observed when lowering the temperature. In contrast, US, for example, is ferromagnetic with a Curie temperature (T_c) of 177 K, and a phase transformation to a rhombohedral structure occurs at lower temperatures.

The high-pressure structural behavior of UP has been studied by Vaidya *et al.*¹ up to 18 GPa and by Leger *et al.*² up to 25 GPa. In the present work we report measurements in the extended-pressure range up to 51 GPa where two phase transitions, similar to those for US (Ref. 3) and UN,⁴ are observed.

II. EXPERIMENTAL PROCEDURE

Uranium monophosphide, UP, was prepared by direct reaction of stoichiometric amounts of the constituents in a sealed tungsten container.⁵ X-ray diffraction studies were performed at DESY-HASYLAB, Hamburg, West Germany, using synchrotron radiation from the storage ring DORIS II. The electron energy was 3.7 GeV in runs dedicated for radiation work and 5.2 GeV in runs for high-energy physics. The diffraction spectra were recorded using the energy-dispersive technique. Experimental details have been published elsewhere.⁴

High pressure up to 51 GPa has been generated in a diamond-anvil cell where an Inconel gasket enclosed the

fine UP powder, the ruby pressure marker, and the pressure-transmitting medium. The latter was either a 4:1 methanol-ethanol mixture or nitrogen. Okai *et al.*⁶ have analyzed different liquid and solid transmitting media and come to the conclusion that the 4:1 methanol:ethanol mixture remains hydrostatic at least up to 20 GPa, i.e., even after the solidification at about 11 GPa. It has been observed⁷ that nitrogen is nearly hydrostatic up to about 13 GPa. Accordingly, in some of our experiments we have loaded the pressure cell in liquid nitrogen.

The pressure was determined by the ruby-fluorescence method using the nonlinear relation⁸

$$P = (380.8 \text{ GPa})[(1 + \Delta\lambda/\lambda_0)^5 - 1],$$

where P is the pressure, $\lambda_0 = 6942.4 \text{ \AA}$ is the wavelength of the ruby R line at ambient pressure, and $\Delta\lambda$ is the pressure-induced wavelength shift.

III. RESULTS

The lattice constant a_0 of cubic UP at ambient pressure and room temperature was determined by high-precision powder diffractometry. The result is

$$a_0 = 5.5844(5) \text{ \AA}.$$

Figure 1 shows examples of energy-dispersive diffraction spectra with the high-pressure cell. The spacing, d , of the lattice planes can be calculated from the energies of the corresponding diffraction peaks knowing the Bragg angle. The latter was determined from a NaCl spectrum. The observed d spacings as functions of pressure are shown in Fig. 2. Three pressure regions can be distinguished. The diffraction lines of the cubic phase ex-

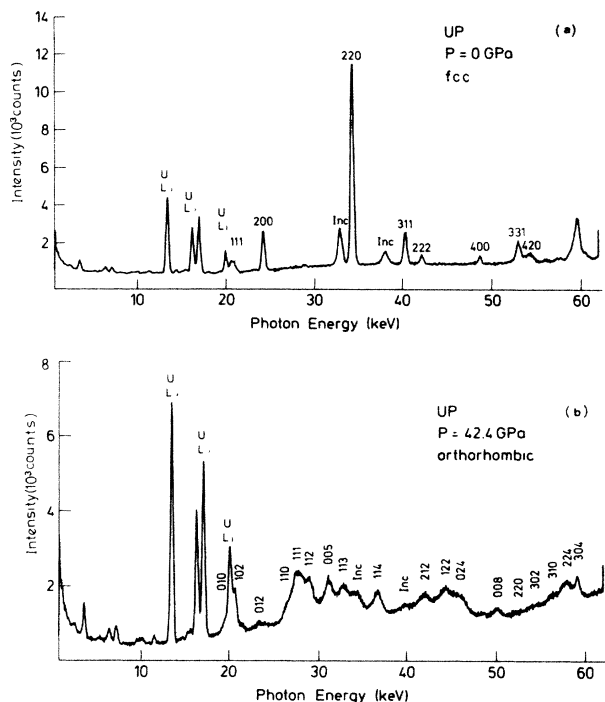


FIG. 1. X-ray energy-dispersive power-diffraction spectra of UP. (a) At atmospheric pressure: fcc phase. (b) At a pressure of 42.4 GPa: orthorhombic phase. Diffraction peaks from the Inconel gasket are denoted Inc. Bragg angle $\theta = 5.25^\circ$.

tend to about 10 GPa. Between 10 and 28 GPa some lines split. Most of the d curves change their slope at 10 GPa, the (200) and (400) curves being notable exceptions. Above 28 GPa several new lines appear. We will denote the two noncubic high-pressure phases UP II and UP III, respectively.

The diffraction lines of UP II can be indexed assuming a rhombohedral distortion of the fcc lattice. Table I lists the calculated and observed d spacings at 16.6 GPa. The goodness of the fit is characterized by a reliability factor $R = 0.23\%$ as defined in Table I. The R value is considered highly satisfactory for a high-pressure energy-dispersive spectrum. Each of the (111) and (220) lines of the cubic phase splits into a pair of lines as seen in Table I and Fig. 2. The separation on the photon-energy scale of the two components of a doublet is less than or equal to the breadth of each line (measured as the full width at half maximum for an x-ray fluorescence line in the same energy range). Therefore, the doublets appear as broad and asymmetric peaks in the raw data. The component lines of the doublets have been resolved by a deconvolution technique using the maximum-entropy principle.¹⁰ Another characteristic feature of the rhombohedral distortion is that it has a negligible effect on the d values of the ($h00$) planes, which explains why the (200) and (400) curves in Fig. 2 are unaffected by the phase transition.

The diffraction lines of UP III have been indexed using an orthorhombic unit cell where $c/a \approx c/b \approx 2\sqrt{2}$, which can be considered as another distorted fcc structure.¹¹ The doubling of the c axis has been done in order to ex-

TABLE I. Rhombohedrally distorted UP at 16.6 GPa: $a = 5.388(13) \text{ \AA}$, $\alpha = 89.4(2)^\circ$. The indices hkl refer to a face-centered rhombohedral unit cell in order to facilitate the comparison with the fcc phase. The indices HKL refer to the conventional triple-hexagonal unit cell (space group $R\bar{3}m$, no. 166). The calculated d spacings have been obtained using the refinement procedure PURUM (Ref. 9). Intensity labels: s denotes strong, m denotes medium, w denotes weak, vw denotes very weak, and t denotes trace (shoulder on a broad peak).

HKL	hkl	d_{calc} (\AA)	d_{obs} (\AA)	Intensity
003	111	3.141	3.145	m
101	$\bar{1}\bar{1}1$	3.101	3.110	t
102	200	2.694	2.687	s
104	220	1.914	1.924	m
110	$2\bar{2}0$	1.896	1.900	t
105	311	1.635	1.631	m
113	$\bar{1}13$	1.623		
201	$\bar{3}11$	1.617		
006	222	1.571	1.569	w
202	$2\bar{2}2$	1.550		
204	400	1.347	1.343	w
107	331	1.245	1.243	w
205	$\bar{1}33$	1.238		
211	$\bar{3}31$	1.230		
116	420	1.209	1.208	vw
122	420	1.200		

$$R = 100 \sum |d_{\text{calc}} - d_{\text{obs}}| / \sum d_{\text{obs}} = 0.23\%$$

plain some of the new lines that are not merely a splitting of the fcc lines. Table II lists calculated and observed d spacings at 42.4 GPa. The R factor of 0.85% is larger than for UP II because of the poorer diffraction data. Therefore, the proposed orthorhombic structure should be considered as an indexing scheme at present, indicating the position of the structure in the symmetry hierar-

TABLE II. Orthorhombic UP III at 42.4 GPa: $a = 3.79(4) \text{ \AA}$, $b = 3.47(2) \text{ \AA}$, $c = 10.75(2) \text{ \AA}$. For intensities, see Fig. 1(b).

hkl	d_{calc} (\AA)	d_{obs} (\AA)
010	3.470	3.480
102	3.102	3.146
012	2.916	2.912
110	2.562	2.569
111	2.492	2.434
112	2.313	2.343
005	2.151	2.170
113	2.084	2.056
114	1.855	1.851
202	1.791	1.777
212	1.591	1.615
122	1.514	1.515
024	1.458	1.470
008	1.344	1.346
310	1.189	1.207
224	1.156	1.172
304	1.145	1.146

$$R = 100 \sum |d_{\text{calc}} - d_{\text{obs}}| / \sum d_{\text{obs}} = 0.85\%$$

chy.¹¹ A similar situation has been found for some other distorted fcc structures suggested for the rare-earths and the actinides.¹² Table III lists the unit-cell dimensions for all measured pressures.

The pressure dependence of the unit-cell volume can be described by a semiempirical equation of state. The experimental data for the cubic phase have been fitted to the Murnaghan and Birch first-order equations,¹³ respectively. The fitting parameters are B_0 and B'_0 , i.e., the isothermal bulk modulus at ambient pressure and its pressure derivative. The Murnaghan equation gives $B_0 = 102.5$ GPa and $B'_0 = 3.9$, the Birch equation $B_0 = 102.1$ GPa and $B'_0 = 4.1$. As a final result we quote

$$B_0 = 102(4) \text{ GPa}, \quad B'_0 = 4.0(8),$$

where the uncertainties are the standard deviations of the least-squares fit to the equation of state.

IV. DISCUSSION

A. Diffraction data

The lattice constant a_0 of cubic UP depends on the stoichiometry. A comparison with published data (Table

IV) indicates that our specimen has the composition UP_x , where $x = 0.98-0.99$. The theoretical a_0 value,¹⁷ calculated at 0 K, is 2% lower than the experimental value. Similar differences are found for other actinide rocksalt-structure compounds.

Table V compares published data for the bulk modulus B_0 and its pressure derivative B'_0 . It is seen that our result is in good agreement with the experimental result of Leger *et al.*,² and with the theoretical calculation of Brooks.¹⁷ The experimental B_0 value reported by Vaidya *et al.*¹ seems to be anomalously high. The pressure-volume data given by these authors correspond to a negative B'_0 value which is unlikely.

The rhombohedral distortion has been observed previously by Leger *et al.*² These authors suggest that one is observing an effect of uniaxial-stress components due to the freezing of the 4:1 methanol-ethanol liquid in the pressure range 10–15 GPa. According to the model devised by Singh and Balasingh,¹⁸ the d spacings are then modified similarly to a rhombohedral distortion. Compared with other uranium compounds UP would be unusually sensitive to uniaxial stress.

It follows from above that one cannot distinguish between a real rhombohedral phase and an apparent distort-

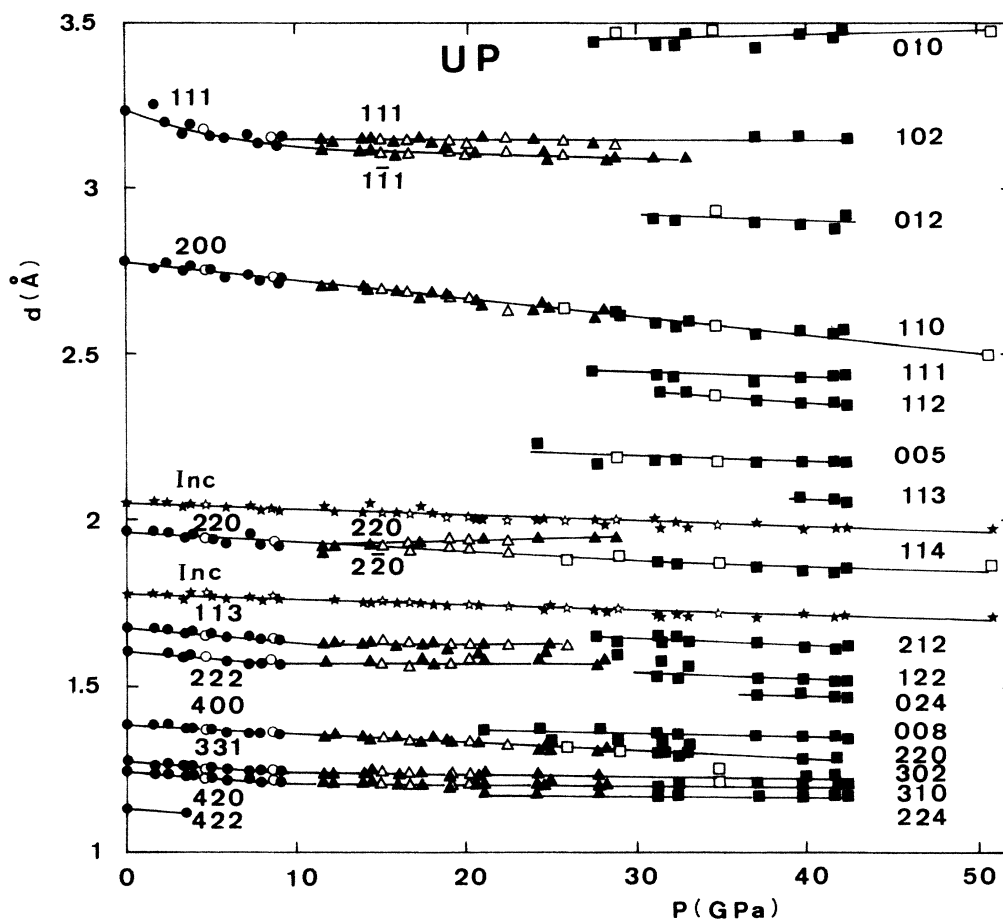


FIG. 2. Interplanar spacings as functions of pressure. The indices based on the fcc unit cell are shown on the left-hand side; those based on the orthorhombic unit cell are on the right-hand side. Circles denote the cubic phase, triangles the rhombohedral phase, squares the orthorhombic phase, and stars the Inconel lines of the gasket. Open symbols refer to the use of nitrogen as the pressure-transmitting medium.

tion due to uniaxial-stress components in the methanol-ethanol mixture. Therefore, we have also made a series of experiments with nitrogen as the pressure-transmitting medium. This should ensure truly hydrostatic pressure in the pressure range of interest here. As seen in Fig. 2, the experimental d values are reproducible and we conclude that we are observing a real phase transformation to rhombohedral UP II.

TABLE III. Unit-cell dimensions for UP. The uncertainties given in parentheses are the standard deviations of the least-squares fit.

P (GPa)	a (Å)		
	Face-centered cubic		
0	5.5844(5) ^a		
0	5.581(5)		
2.45	5.542(5)		
3.77	5.518(3)		
4.55	5.508(9)		
5.07	5.496(3)		
5.94	5.481(4)		
7.24	5.465(6)		
7.86	5.455(8)		
8.98	5.446(12)		
9.20	5.440(12)		
	a (Å)	α (deg)	
	Rhombohedral		
11.6	5.41(1)	89.4(1)	
13.9	5.40(1)	89.5(2)	
14.3	5.39(1)	89.2(2)	
15.0	5.41(2)	89.6(2)	
15.9	5.38(2)	89.4(5)	
16.6	5.39(2)	89.4(2)	
17.0	5.38(2)	89.2(2)	
17.3	5.36(2)	88.7(3)	
18.8	5.35(2)	89.3(2)	
19.0	5.36(2)	89.2(2)	
20.1	5.36(2)	88.6(3)	
21.1	5.34(3)	88.3(5)	
22.2	5.34(5)	89.0(9)	
24.1	5.32(4)	88.1(7)	
	a (Å)	b (Å)	c (Å)
	Orthorhombic		
27.6	3.85(2)	3.55(3)	10.95(4)
28.9	3.82(3)	3.58(3)	10.95(7)
31.1	3.86(3)	3.51(2)	10.97(3)
32.3	3.87(3)	3.48(2)	10.89(3)
34.7	3.91(9)	3.48(5)	10.87(7)
37.0	3.82(4)	3.50(2)	10.85(2)
40.0	3.81(4)	3.49(2)	10.82(3)
41.6	3.79(4)	3.49(3)	10.79(3)
42.4	3.79(4)	3.47(2)	10.75(2)
50.8	3.59(15)	3.46(15)	10.9(3)

^aDetermined by precision diffractometry.

TABLE IV. Lattice constant a_0 of cubic UP at ambient pressure and room temperature.

a_0 (Å)	Compos.	Ref.	Remarks
5.5844		this work	
5.584	UP _{0.98}	14	
5.586	UP _{0.99}	14	
5.589	UP _{1.00}	14	
5.5888(1)	UP	15	
5.5888(2)	UP	16	Prep. by diffusion process
5.5882(2)	UP	16	Prep. by exothermal process
5.46	UP	17	Theor. value

Figure 3 shows the relative volume of UP as a function of pressure. The curve for the cubic phase has been calculated from the equation of state. It is seen that the volume versus pressure is described by a continuous curve in the whole pressure range. There are no volume discontinuities at the phase transitions.

B. Influence of the electronic structure

The ordering temperatures and magnetic moments of metallic compounds are sensitive to volume in a manner summarized in the Hill plots.¹⁹ For uranium compounds there is a transition region for a U-U distance of about 3.4 Å, below which one expects nonmagnetic behavior and delocalization of the 5*f* electrons.

The U-U separation in cubic UP is 3.95 Å at ambient pressure and 3.85 Å when the transition to rhombohedral UP II occurs at 10 GPa. The U-U distance has decreased to 3.76 Å at 28 GPa where the transition to orthorhombic UP III takes place. At the maximum pressure, 51 GPa, in the present work the U-U separation is 3.46–3.59 Å measured in the (001) plane of the orthorhombic unit cell. Thus the U-U distance is above the

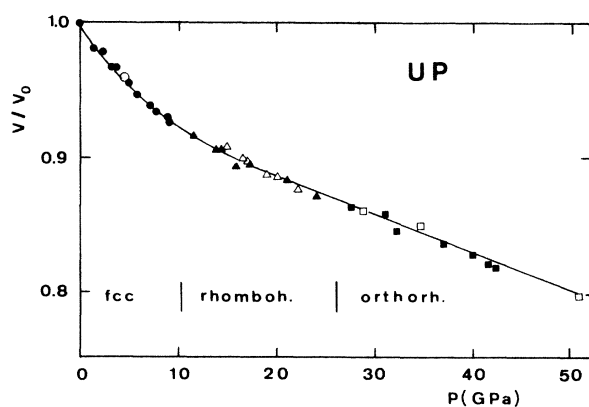


FIG. 3. Relative volume of UP as a function of pressure. The curve for the fcc phase (< 10 GPa) has been calculated from the equation of state. The symbols are the same as in Fig. 2.

TABLE V. The bulk modulus B_0 of cubic UP and its pressure derivative B'_0 at ambient pressure. The uncertainties, given in parentheses, are the standard deviations of the least-squares fit to the equation state.

B_0 (GPa)	B'_0	Ref.	Pressure region
102(4)	4.0(8)	this work	$p \leq 10$ GPa
250(10)	<0	1	$p \leq 18$ GPa
102(3)	4.7(5)	2	$p \leq 25$ GPa
107		17	Theor. value

critical value 3.4 \AA in the whole pressure range investigated.

In comparison, UC and UN have the smallest anions and therefore the smallest U-U separation of the uranium rocksalt-structure compounds. High-pressure studies have shown that UC (Ref. 20) and UN (Ref. 4) transform to distorted fcc structures when the U-U distance is $3.34\text{--}3.38 \text{ \AA}$, i.e., just below the critical value in the Hill plot. The transitions are of first order with a volume collapse of 3–5%. The corresponding thorium compounds, ThC (Ref. 21) and ThN (Ref. 22), have no phase transformations and remain cubic in the same pressure range. UAs, USe, USb, and UTe have larger anions and correspondingly larger U-U separation. These compounds are all found to transform to the CsCl-type structure ($B2$) at high pressure with a volume collapse of about 10%.²³ The same transformations are found for the corresponding thorium compounds as well as ThP.²³

From high-pressure studies on the rare-earth metals it is now understood that the s and d electrons are responsible for high-symmetry structures (hcp, Sm type, dhcp, and fcc), whereas the f electrons tend to favor distorted structures as seen in the case of cerium (e.g., Ref. 24).

A similar correlation between crystal structure and electronic structure has been found for the actinide met-

als. Thorium has the high-symmetric fcc structure in accordance with the $5f$ band of thorium being essentially unoccupied. Uranium, on the other hand, has about three $5f$ electrons which are nonlocalized (itinerant) and contribute to the metallic bonding. Consequently, uranium has a low-symmetric structure (orthorhombic α -U).

Proceeding along the actinide series in the Periodic Table it is not until americium that one again finds high-symmetric structures similar to those of the rare earths. In the heavy actinides the $5f$ electrons are localized and do not participate in the metallic bonding.

From the evidence above we conclude that the transformation to the CsCl-type structure observed for the large anion uranium and thorium compounds is determined by the $7s$ and $6d$ electrons of the actinide, possibly together with the electrons of the ligand. The transformation of the small-anion uranium compounds is determined by the influence of the $5f$ electrons. The structural stability of the small-anion thorium compounds is explained by their low $5f$ occupation number.

The phase transformations of UP reported in the present work do not fall into one or the other of the categories discussed above. The distorted structures of UP II and UP III indicate an influence of the f electrons. However, the U-U separation is above the critical value of the Hill plot, indicating that the s and d electrons also have some influence on the transitions. Absorption-edge measurements at high pressure would be useful to determine possible valence changes in uranium at the phase transformations of UP.

ACKNOWLEDGMENTS

We wish to express our thanks to DESY-HASYLAB for the permission to use the synchrotron-radiation facility. Financial support from the Danish Natural Science Research Council is gratefully acknowledged.

¹S. N. Vaidya, C. Karunakaran, M. D. Karkhanavala, and R. Krishnan, *J. Nucl. Mater.* **60**, 339 (1976).

²J. M. Leger, K. Oki, A. M. Redon, I. Vedel, J. Rossat-Mignod, and O. Vogt, *Phys. Rev. B* **33**, 7205 (1986); I. Vedel, K. Oki, A. M. Redon, R. M. Leger, J. Rossat-Mignod, and O. Vogt, *J. Less-Common Met.* **121**, 157 (1986); I. Vedel, A. M. Redon, and J. M. Leger, *Physica B + C* **144B**, 61 (1986).

³J. Staun Olsen, S. Steenstrup, L. Gerward, U. Benedict, J. C. Spirlet, and G. D. Andreotti, *J. Less-Common Met.* **98**, 291 (1984), and unpublished.

⁴J. Staun Olsen, L. Gerward, and U. Benedict, *J. Appl. Crystallogr.* **18**, 37 (1985).

⁵K. Mattenberger, L. Scherrer, and O. Vogt, *J. Cryst. Growth* **67**, 467 (1984).

⁶B. Okai, O. Shimomura, and I. Fujishiro, *Physica B + C* **139&140B**, 799 (1986).

⁷R. Le Sar, S. A. Ekberg, L. H. Jones, R. L. Mills, L. A. Schwalbe, and D. Schiferl, *Solid State Commun.* **32**, 131 (1979).

⁸H. K. Mao, P. M. Bell, J. Shaner, and D. J. Steinberg, *J. Appl. Phys.* **49**, 3276 (1978).

⁹P. E. Werner, *Ark. Kemi* **31**, 513 (1969).

¹⁰S. Steenstrup, *Aust. J. Phys.* **38**, 319 (1985).

¹¹L. Gerward, J. Staun Olsen, and U. Benedict, *Physica B + C* **144B**, 72 (1986).

¹²S. K. Sikka and V. Vijayakumar, *Physica B + C* **144B**, 23 (1986).

¹³See, for example, C. S. Menoni and I. L. Spain, in *High Pressure Measurement Techniques*, edited by G. N. Peggs (Applied Science, London, 1983), p. 133.

¹⁴Y. Baskin, *J. Am. Ceram. Soc.* **49**, 541 (1966).

¹⁵O. L. Kruger and J. B. Moser, *J. Phys. Chem. Solids* **28**, 2321 (1967).

¹⁶J. L. Driscoll and P. E. Evans, *J. Nucl. Mater.* **28**, 311 (1968).

¹⁷M. S. S. Brooks, *J. Phys. F* **14**, 653 (1984).

¹⁸A. K. Singh and C. Balasingh, *J. Appl. Phys.* **48**, 5338 (1977).

¹⁹H. H. Hill, *Nucl. Metall.* **17**, 2 (1971).

²⁰J. Staun Olsen, L. Gerward, U. Benedict, J.-P. Itié, and K.

- Richter, J. *Less-Common Met.* **121**, 445 (1986).
- ²¹L. Gerward, J. Staun Olsen, U. Benedict, J.-P. Itié, and J. C. Spirlet, *J. Appl. Crystallogr.* **19**, 308 (1986).
- ²²L. Gerward, J. Staun Olsen, U. Benedict, J.-P. Itié, and J. C. Spirlet, *J. Appl. Crystallogr.* **18**, 339 (1985).
- ²³J. Staun Olsen, L. Gerward, S. Dabos, U. Benedict, O. Vogt, and J. C. Spirlet (unpublished).
- ²⁴B. Johansson, *J. Magn. Magn. Mater.* **47&48**, 231 (1985).